Open Access

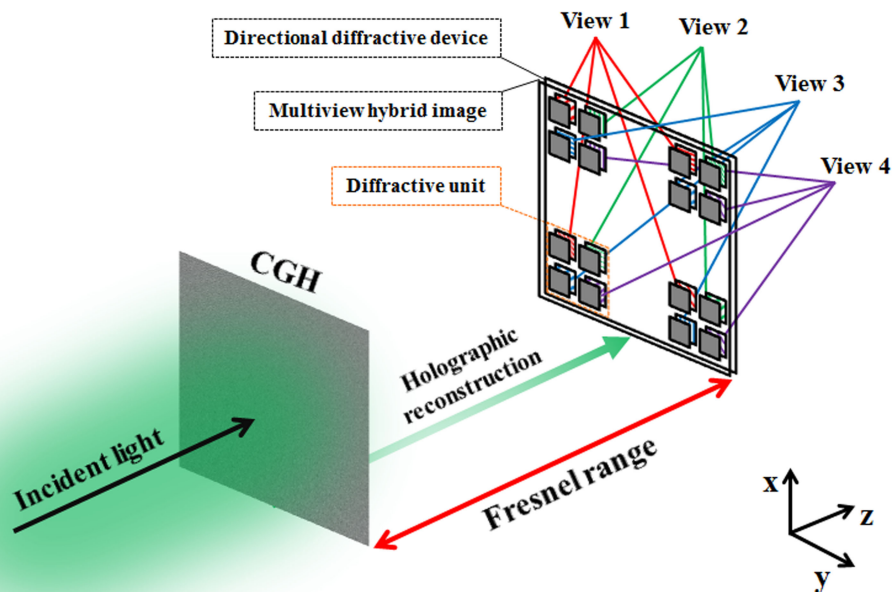# Projection-Type Multiview Holographic Three-Dimensional Display Using a Single Spatial Light Modulator and a Directional Diffractive Device

Yanfeng Su
Zhijian Cai
Kai Wu
Lingyan Shi
Feng Zhou
Haidong Chen
Jianhong Wu

Projection-Type Multiview Holographic Three-Dimensional Display Using a Single Spatial Light Modulator and a Directional Diffractive Device

Yanfeng Su [ID] **, Zhijian Cai, Kai Wu, Lingyan Shi, Feng Zhou, Haidong Chen, and Jianhong Wu**

School of Optoelectronic Science and Engineering and Collaborative Innovation Center of Suzhou Nano Science and Technology and Key Lab of Advanced Optical Manufacturing Technologies of Jiangsu Province and Key Lab of Modern Optical Technologies of Education Ministry of China, Soochow University, Suzhou 215006, China

Abstract: In this paper, we propose a projection-type multiview holographic three-dimensional (3-D) display using a single spatial light modulator (SLM) and a directional diffractive device, where a phase-only Fresnel hologram is calculated and displayed on the SLM to reconstruct the multiview hybrid image of a 3-D object for providing the amplitude information of a multiview light field, and a directional diffractive device covered with many pixelated gratings is designed to guide different reconstructed perspectives into different viewing zones for expressing the phase information of the light field. Furthermore, a four-view directional diffractive device is fabricated by using the pixelated holographic exposure method, and its optical properties are also measured under a collimated illumination of the green reconstruction laser with the designed wavelength. In addition, an experimental verification system is constructed to demonstrate a four-view 3-D display. The recorded experimental results confirm that a crosstalk-free four-view light field is created, which is beneficial from the precise alignment between the directional diffractive device and the reconstructed image. Moreover, the capability of dynamic display with the proposed system is also tested by refreshing the SLM with the sequential holograms, and the captured videos show a promising potential for the real-time multiview holographic 3-D projectors.

Index Terms: Three-dimensional display, holographic display, computer holography, spatial light modulator, diffraction grating.

1. Introduction

Three-dimensional (3D) displays have attracted wide attention because they can provide 3D sensation close to the real life, especially in the fields of medical health [1], [2], digital signage [3], [4], and entertainment [5], [6]. In recent years, with advances in optoelectronic display technology and computer science, many kinds of techniques have been proposed to realize 3D displays, where stereoscopic display represented by stereoscopic glasses has rapidly developed and gradually

formed a commercial scale in 3D movies or games owing to its shocking 3D effect. However, the observer needs to wear special eyewear for watching the stereo images, and the inconvenience of having to wear auxiliary greatly limits its applications in many 3D visualization areas [7]. Alternatively, glasses-free 3D display techniques have increasingly been studied for providing a better observation experience. Holography is regarded as the most promising technique for realizing glasses-free 3D display that can present a true 3D image for human eyes with all depth cues. In an optical hologram, both the amplitude and phase information of the 3D object are recorded on the holographic recording media via the interference between object and reference light for photorealistic 3D reconstruction, while the refreshable rate of the current available holographic recording media still cannot satisfy the requirement of real-time 3D display [8]. Besides, electronic holography based on spatial light modulator (SLM) is another approach to realize holographic 3D display, where computer-generated holograms (CGHs) that are flexibly encoded by simulating light propagation and interference on computers can be sequentially displayed on the SLM for dynamic 3D reconstruction. Compared with the optical holography, the holographic display with CGHs has the advantages of fast refresh rate, high flexibility of hologram generation, and avoiding the uses of holographic recording medium and optical path so that more and more researches in the dynamic holographic 3D display focus on the SLM-based electronic holography [9]–[12]. However, the satisfactory holographic 3D video display may hardly be achieved by using the current available SLM, where the major limitation is the low space bandwidth product (SBP) of the state-of-the-art SLM caused by the overlarge pixel pitch and the inadequate pixel number [13]–[16]. To enhance the low SBP of a single SLM, many spatial [17]–[19] or time [20], [21] multiplexing methods have been proposed, but they usually require multiple SLMs or a SLM with the requirement of ultrahigh refresh rate, resulting in a significantly increased complexity and cost of the system. Moreover, the huge calculated and refreshable data volume of the wavefronts of the 3D objects could also increase the difficulty of real-time holographic 3D display.

In practice, autostereoscopic multiview 3D display shows its merits of low cost, simple fabrication, small refreshable data volume, and good compatibility with current two-dimensional (2D) display techniques [22]–[24]. To date, many realization methods about multiview 3D display have been proposed and studied widely, and they can be largely classified into the pure geometrical optics method and the diffractive optics method. In general, the pure geometrical optics method employs parallax barrier, lenticular, micro lens, or directional backlight as the light-guide element [25]–[29], and the 3D perception could be achieved by combining the light-guide element and the liquid crystal display (LCD) with a precise alignment. But the method has several drawbacks of reduced light efficiency, excessive crosstalk, and limited resolution. Furthermore, multiple projectors solutions [30]–[32] have also been introduced to overcome the resolution limitation at the expense of system portability and compactness.

Another kind of method for multiview 3D display is based on diffractive optics, one of the solutions is holographic stereogram composed of many holographic pixels, namely, hogels. The holographic stereogram is generated accordingly by multiple discrete 2D perspectives of a 3D object, and each hogel in holographic stereogram records both amplitude and phase information of object wave, where the recorded phase information is expressed as the holographic fringe patterns or grating patterns. Thus, a holographic stereogram can cause a particular perspective image to be viewed only from a particular viewing angle because the incident light is modulated by grating patterns with different grating vectors, which may be easier to reconstruct dynamic 3D images thanks to its greatly reduced data volume compared with the true 3D holographic display. To generate updatable holographic stereograms, Savas Tay *et al.* [33] used photorefractive polymers as dynamic holographic recording materials for optical holography, and then P.-A. Blanche *et al.* from the same group [34] optimized the previous architecture to achieve a multichannel read-and-write. However, the refreshable rate is still not fast enough to achieve real-time display. In addition, Mark Lucente *et al.* [35] computed the holographic stereograms for real-time 3D display by using a series of basis fringes to control the directional propagation of the diffracted light, but the final display quality is severely limited by the adopted SLM, especially the small diffraction angle and the narrow observation range.

Except for the solution of holographic stereogram, several groups recently proposed a pixelated diffractive element [36] for directionally guiding the diffracted light to realize multiview 3D display. David Fattal *et al.* [37] proposed and fabricated a grating-based directional backlight structure to create a wide-angle full parallax multiview lightfield, where the directional backlight structure composed of diffractive grating pixels can re-direct the incident light into multiple viewing directions. Nevertheless, the crosstalk between viewing zones is difficult to avoid completely because of the fixed spatial frequency and orientation of the diffractive grating pixels, and the size of the fabricated structure is severely limited due to the use of E-beam writing lithography. In order to solve these two problems, Wenqiang Wan *et al.* [38] proposed a continuously variable spatial frequency lithography system to efficiently fabricate the diffractive element consisting of grating pixels, where the period of the fabricated grating pixel can be varied with a step length of 1 nm. Later, they combined the fabricated diffractive element with a LCD to realize multiview dynamic 3D display [39]. For the point-to-point imaging with LCD, however, the final display images will seriously affected by the partial pixel defect, especially the defective points after using for a long time, while the influence of the partial pixel defect can be significantly weakened and the defective points can be avoided in the holographic reconstruction with SLM because each pixel in the reconstructed image plane can be regarded as a comprehensive contribution of all of sampling units on the hologram plane. So, in this paper, we propose a projection-type multiview holographic 3D display using a single SLM and a directional diffractive device, where the SLM is adopted to display a phase-only Fresnel hologram for reconstructing the amplitude information of multiple perspectives of a 3D object, and the directional diffractive device is employed to guide different reconstructed perspectives into different viewing zones for providing the phase information of multiview lightfield. The phase-only hologram is calculated accordingly by the multiview hybrid image of the 3D object. The grating vector of each grating pixel in the directional diffractive device, including the period and orientation, is carefully designed based on diffractive optics, and then the directional diffractive device is fabricated on the photoresist pixel by pixel. Furthermore, the diffraction properties of the fabricated directional diffractive device are measured by using a green laser with the wavelength of 532 nm as the illuminating light. Thereafter, by optically reconstructing the pre-calculated phase-only Fresnel hologram with the SLM, each reconstructed perspective can be presented at corresponding viewing point only, which leads to crosstalk-free multiview lightfield. Moreover, dynamic multiview holographic 3D display is also realized by refreshing the adopted SLM with the sequential holograms.

2. System and Principle

Figure 1 schematically shows the proposed projection-type multiview holographic 3D display. The information source is the multiple 2D perspectives of a 3D object, and the perspectives with parallax can be obtained by 3D computer graphic or captured by real 3D model using camera array. Then the obtained perspectives will be pre-processed to the multiview hybrid image with the interweaving arrangement method for hologram calculation. Subsequently, for the hologram plane, the complex amplitude distribution $U(x, y)$ contributed by the multiview hybrid image can be calculated by the Fresnel diffraction formula [40]:

$$U(x, y) = \frac{1}{j\lambda z} \exp(jkz) \iint A(\xi, \eta) \exp[j\varphi(\xi, \eta)] \exp\left\{j\frac{\pi}{\lambda z}\left[(x - \xi)^2 + (y - \eta)^2\right]\right\} d\xi d\eta \qquad (1)$$

where $j, \lambda, z, A(\xi, \eta)$, and $\varphi(\xi, \eta)$ are the imaginary unit, the wavelength, the distance between the hologram plane and the multiview hybrid image plane, the amplitude distribution of the multiview hybrid image plane, and the random phase distribution for smoothening the spatial spectrum of the object information, respectively. After keeping the phase of the complex amplitude distribution calculated above only and removing the amplitude, the phase-only Fresnel hologram of the multiview hybrid image can be obtained as follows:
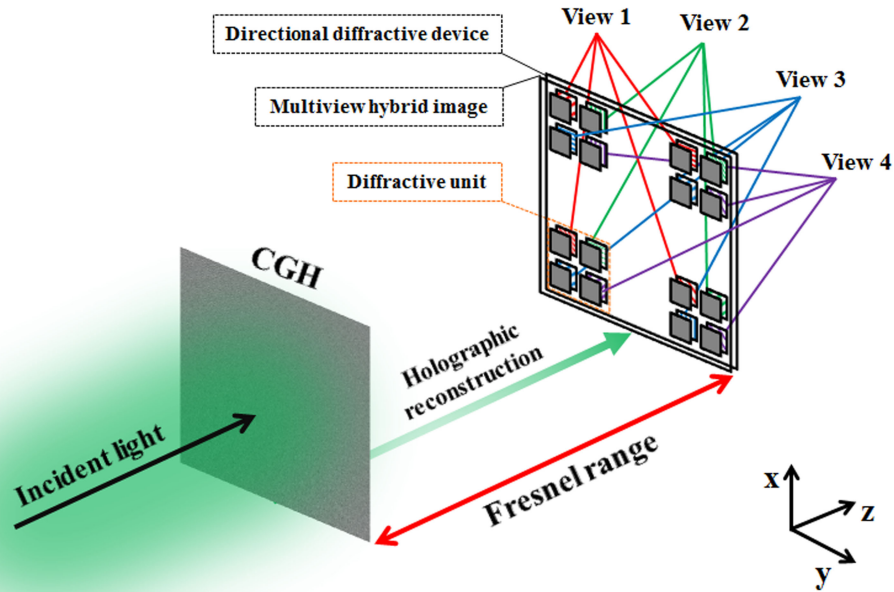
$$H(x, y) = \arg[U(x, y)] \qquad (2)$$

Fig. 1. Schematic of the proposed projection-type multiview holographic 3D display.

where $H(x, y)$ and arg represent the phase distribution of the calculated hologram and the argument operation, respectively. Finally, the calculated hologram would be uploaded onto a phase-only SLM for optical holographic reconstruction, which provides the amplitude information of multiview lightfield.

During the optical reconstruction with the pre-calculated hologram above, the sampling number of the hologram loaded on the SLM is equal to the pixel number of the holographic reconstructed image according to the Nyquist sampling theorem. Assume that the horizontal and vertical sampling numbers of the hologram plane are M, N, and the horizontal and vertical pixel pitches of the adopted SLM are Δx, Δy, respectively. Thus, the horizontal and vertical sizes of the reconstructed image are determined by $\lambda z / \Delta x$ and $\lambda z / \Delta y$, respectively. Therefore, the horizontal and vertical pixel pitches of the reconstructed image can be calculated by:

$$\Delta \xi = \frac{\lambda z}{M \Delta x}$$

$$\Delta \eta = \frac{\lambda z}{N \Delta y} \tag{3}$$

In addition, a directional diffractive device composed of pixelated gratings with various grating vectors is placed at the reconstructed image plane, which is used to express the phase information of multiview lightfield by re-directing the incident light to multiple viewing zones. Generally, R grating pixels with R different grating vectors make up a diffractive unit in the R-view directional diffractive device, where each grating pixel will modulate a corresponding reconstructed image pixel with a special diffracted direction, which is depicted in Fig. 1 by taking 4-view for example. Assume that the directional diffractive device contains S diffractive units, there will be $R \times S$ grating pixels in total, and these grating pixels are matched with the valid pixels of the reconstructed image one by one, where the valid pixels represent the illuminated image pixels for multiview display. Thus, the pixel number of the final each view will be S.

Moreover, in order to create a multiview lightfield, it is necessary that the period and orientation of each grating pixel are designed by the diffraction theory. Figure 2 schematically illustrates the interference pattern generation and directional light-guide process of a grating pixel based on
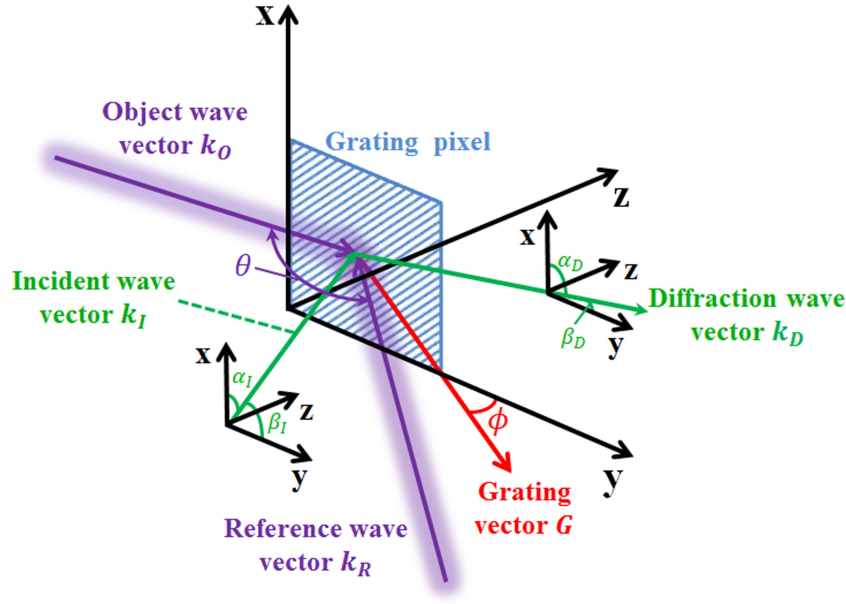
Fig. 2. Interference pattern generation and directional light-guide process of a grating pixel.

holographic recording and readout theory [38], [41]. Two recording plane wave beams, object wave and reference wave, illuminate the glass substrate which is covered by photoresist with an included angle of θ simultaneously for grating pattern generation. The relationship between the two recording waves and the grating can be written as:

$$k_O - k_R = G \tag{4}$$

where k_O, k_R, and G are the object wave vector, the reference wave vector, the grating vector, respectively, and $|G| = 2\pi/\Lambda$, Λ represents the period of the grating. When a readout beam is incident on the recorded grating, the first-order diffraction beam can be calculated by:

$$k_D = k_I - G \tag{5}$$

where k_I and k_D are the incident readout wave vector and the diffraction wave vector, respectively, and $|k_I| = n2\pi/\lambda$, $|k_D| = 2\pi/\lambda$, n represents the refractive index of the directional diffractive device. From Eq. (5), the period Λ of the grating can be deduced by:

$$\Lambda = \sqrt{\frac{\lambda^2}{(n\cos\alpha_I - \cos\alpha_D)^2 + (n\cos\beta_I - \cos\beta_D)^2}} \tag{6}$$

where α_I, β_I are the included angles between the incident wave vector and x axis, y axis, respectively; α_D, β_D are the included angles between the diffraction wave vector and x axis, y axis, respectively.

The orientation angle ϕ of the grating vector from the y axis could also be obtained as follows:

$$\phi = \arctan\frac{n\cos\beta_I - \cos\beta_D}{n\cos\alpha_I - \cos\alpha_D} \tag{7}$$

For each grating pixel in the directional diffractive device, its own position in the directional diffractive device and the predefined position of the corresponding viewing point directly determine the diffraction wave vector of the grating pixel such that the period and orientation angle of each grating pixel can be calculated according to Eq. (6) and Eq. (7).

Furthermore, in order to effectively avoid the unfavorable crosstalk problem, the grating pixels in the directional diffractive device need to be well aligned with the valid pixels in the reconstructed

image one by one, which depends on the six-dimensional (6D) precise adjusting device and the added digital grating on the pre-calculated phase-only Fresnel hologram, and the former and the latter control the movements of the directional diffractive device and the reconstructed image, respectively. In such a way, a crosstalk-free multiview lightfield is created and the parallax images observed at two viewing points will form a stereoscopic image for observer. However, because of the pixelated structure of the used SLM, there exists the undesirable light in the holographic reconstruction [42]–[44]. In order to eliminate the undesirable light, the off-axis holographic reconstruction is firstly realized thanks to the added digital grating mentioned above. Subsequently, a band-pass filter is set before the directional diffractive device in the reconstructed optical path for allowing the desirable reconstructed image to pass through only such that the holographic reconstruction without the undesirable light is generated for the final multview 3D display. Moreover, dynamic 3D display based on the SLM and the directional diffractive device can also be achieved by sequentially refreshing multiple pre-calculated holograms only.

3. Experiments and Results

In the following experiments, a green laser with the wavelength of 532 nm is employed as the illuminating light source, and a reflective-type SLM (Holoeye Pluto VIS-016) with the pixel number of 1920 $\times$ 1080 and the pixel pitch of 8 μm is used to load the phase-only Fresnel holograms for optical reconstruction. The reconstruction distance is assumed as 900 mm, hence the size of the reconstructed image is 59.85 mm $\times$ 59.85 mm, and the horizontal and vertical pixel pitches of the reconstructed image are 31.172 μm and 55.417 μm, respectively. We design a 4-view directional diffractive device with the angle separation of 6$°$ and the total grating pixel number of 60 $\times$ 60 to verify the feasibility of the proposed method, where the pitch of two adjacent grating pixels is 997.5 μm and a diffractive unit contains 2 $\times$ 2 grating pixels, thus the final each view will be consisted of 30 $\times$ 30 pixels. Furthermore, the best viewing distance is set at 300 mm from the directional diffractive device. Therefore, the 4-view directional diffractive device is composed of pixelated gratings with varying periods from 946 nm to 1841 nm.

3.1 Fabrication and Measurement of the Directional Diffractive Device

The pixelated holographic exposure method is employed to fabricate the designed 4-view directional diffractive device on the photoresist (RJZ-390), and the used photolithography setup is the continuously variable spatial frequency lithography system (SVG Corporation, Nanocrystal200), whose fabrication capability for pixelated grating array has been sufficiently proved as several works previously reported [38], [39]. During the fabrication experiment of the 4-view directional diffractive device, a laser with the wavelength of 351 nm is used as the recording light source for performing the holographic exposure pixel by pixel, and the photoresist sample coated on the BK9 glass substrate is fixed on a monitored stage, where the stage will precisely shift a tiny step after recording one grating pixel and before recording the next grating pixel. Furthermore, the fabricated speed of the directional diffractive device is 40 mm^2/mins, which is much faster than the E-beam lithography. Thereafter, the sample is developed in NaOH solutions and subsequently dried by electric blow drier. In such a way, the 4-view directional diffractive device is fabricated, whose actual photograph is presented in Fig. 3(a). Moreover, the surface morphology of the fabricated directional diffractive device on the photoresist is characterized by the scanning electron microscopy (SEM), and corresponding photos are depicted in Figs. 3(b) and 3(c). In addition, the size of each grating pixel in the fabricated directional diffractive device is 150 μm $\times$ 150 μm, smaller than the pitch of two adjacent grating pixels, which provides an operation tolerance when aligning the directional diffractive device with the reconstructed image.

Furthermore, the optical properties of the fabricated 4-view directional diffractive device are measured under the collimated illumination of the green laser mentioned above. Figure 4(a) shows the viewing point separation of the fabricated directional diffractive device. The collimated light is focused to four light spots, which represent four different viewing points (view 1–4), and the
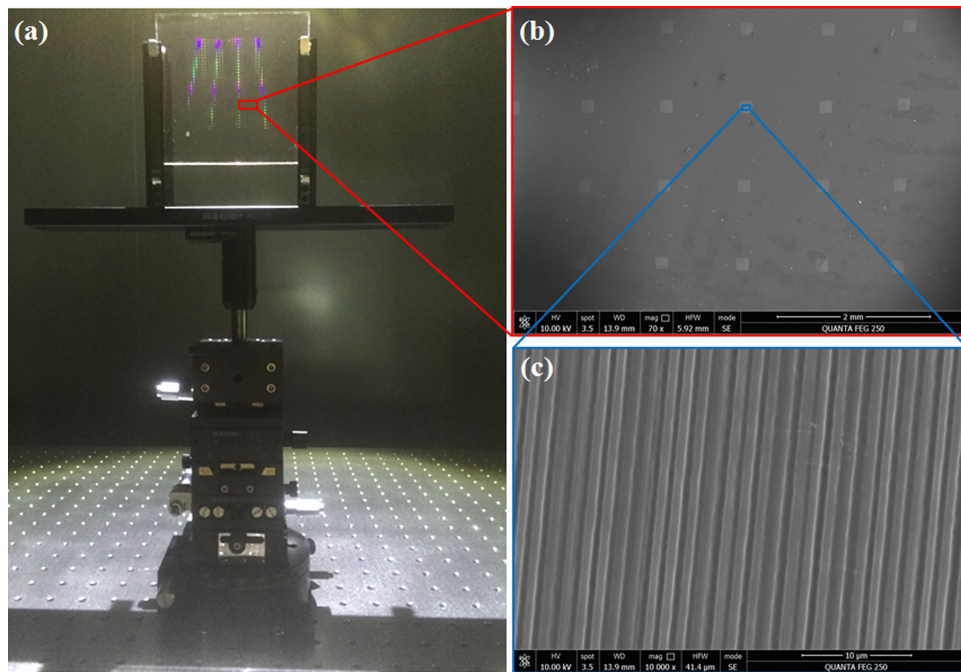
Fig. 3. (a) Photograph of the fabricated 4-view directional diffractive device fixed in the 6D adjusting device. (b) The SEM photo of the fabricated directional diffractive device with pixelated grating array. (c) The partial enlargement of SEM photo of a pixelated grating.
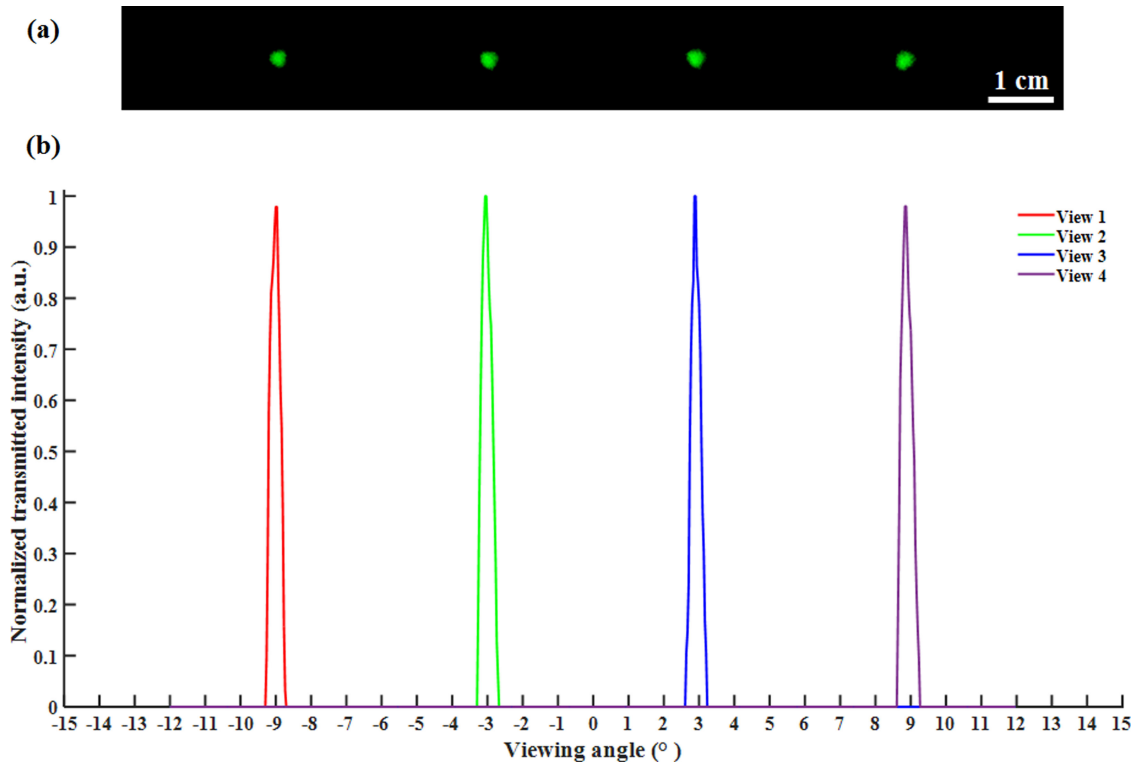

Fig. 4. (a) The viewing point separation of the fabricated 4-view directional diffractive device. (b) The normalized intensity distribution of these four viewing points.
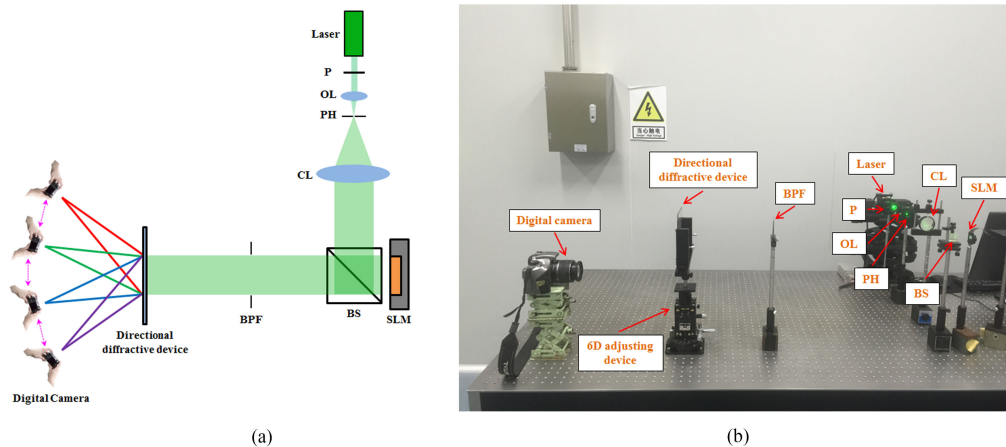
Fig. 5. (a) Schematic illustration and (b) experimental setup for the proposed projection-type multiview holographic 3D display system. P: polarizer, OL: objective lens, PH: pinhole, CL: collimating lens, BS: beam splitter, BPF: band-pass filter.

measured distance between the viewpoint plane and the directional diffractive device is 300 mm, which is same as the best viewing distance designed above. Moreover, the diffraction efficiency of the 4-view directional diffractive device is also measured, and the measurement results about actual diffraction efficiency are shown as follows: 5.0% for the view 1; 5.2% for the view 2; 5.2% for the view 3; and 5.1% for the view 4. Besides, the normalized intensity distribution of these four viewing points is illustrated in Fig. 4(b). From Fig. 4(b), we can see that the four viewing points distribute uniformly from $-9°$ to $9°$, and the angle separation between the adjacent viewing points is equal to $6°$, revealing a good consistency with the theoretical design of four viewing points. Meanwhile, the average angular divergence of the four viewing points is measured as 0.23 degree (FWHM), which is slightly larger compared with the diffraction limit (0.18 degree).

3.2 Experimental Verification of the Proposed Projection-Type Multiview Holographic 3D Display

In order to demonstrate the proposed projection-type multiview holographic 3D display, an experimental verification system is constructed, whose schematic illustration and experimental setup are shown in Figs. 5(a) and 5(b), respectively. It consists of a green laser mentioned above, a polarizer, an objective lens for expanding the laser beam, a pinhole, a collimating lens for generating the plane wave, a beam splitter, the SLM mentioned above, a band-pass filter, the fabricated 4-view directional diffractive device fixed in the 6D adjusting device with an adjusting accuracy of $10\,\mu$m, and a digital camera (Canon EOS 300D) for recording the displayed images. According to the design of pixelated gratings in the 4-view directional diffractive device, four perspectives of a 3D object is firstly pre-processed to a 4-view hybrid image with the interweaving arrangement method, and then the phase-only Fresnel hologram of the 4-view hybrid image is calculated and displayed on the SLM for holographic reconstruction. Subsequently, in the experimental setup shown in Fig. 5, the fabricated 4-view directional diffractive device fixed in the 6D adjusting device is set at 900 mm from the SLM, and the distance is equal to the reconstruction distance. Finally, the reconstructed hybrid image is separated into four different viewing points after aligning the reconstructed image with the directional diffractive device. As aforementioned, the crosstalk-free 4-view lightfield is created.

To test the independence of the diffracted light beams for forming four separated viewing points, the four characters ("1," "2," "3," "4") are employed to project to the four different viewing points, respectively. Then the phase-only Fresnel hologram is generated by using the four characters as the four perspectives, which is shown in Fig. 6(a). Subsequently, the calculated hologram is displayed on the SLM, and the 4-view reconstruction results are also recorded by moving the
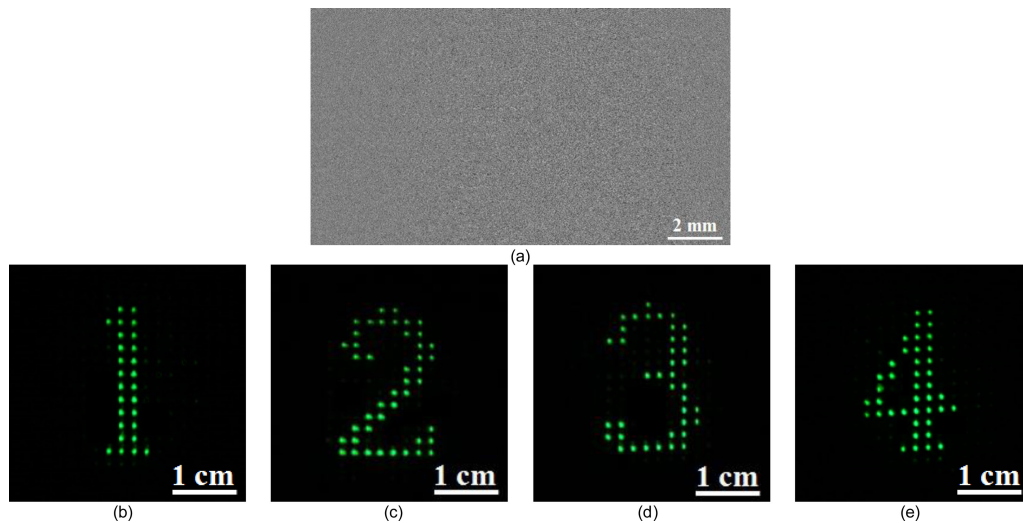
Fig. 6. (a) Calculated phase-only Fresnel hologram, and (b)–(e) are the recorded reconstructed images at four different viewing points, respectively.
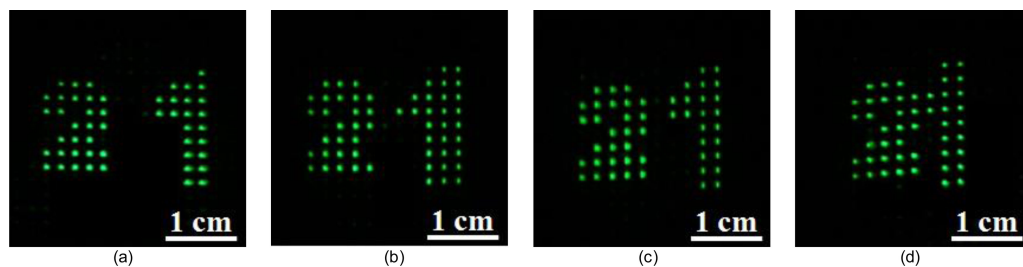

Fig. 7. (a)–(d) are the recorded reconstructed images of two characters ("1" and "2") at four different viewing points, respectively. Rotating characters, "1" and "2" (see media 1–4 and media 5–8).

digital camera, which are shown in Figs. 6(b)–(e), respectively. From the recorded results shown in Figs. 6(b)–(e), it is clearly seen that there are no crosstalk and ghost effect when observing at the four viewing points, proving the good independence of the diffracted light beams for forming four different viewing points.

Furthermore, a virtual 3D object consisting of two characters ("1" and "2") in different depths is designed in Autodesk 3ds Max to realize 4-view 3D display. Four perspectives of the 3D object are firstly obtained by setting a camera array in the software, and the subsequent procedures are same as the processing procedures of the four characters mentioned above. Figure 7 shows the recorded results from four various viewing points, and two of the parallax images form a stereoscopic image. Obviously, character "1" is nearer than the character "2" from the observer. Moreover, the character "1" and the character "2" rotate around the geometric center of central depth plane by refreshing the SLM with the sequential holograms at a refresh frame rate of 20 fps, and the dynamic scene can also be observed and captured at four viewing points. The demo videos captured in the dark condition and the ambient light are shown in media 1–4 and media 5–8, respectively. Analogously, the rotating characters ("3" and "D") are also sequentially reconstructed to four viewing points, and corresponding dynamic reconstructed images are captured in the dark condition and shown in media 9–12, respectively. When the refreshing hologram is stopped in one of the video frames, the 4-view images are also recorded at the predefined four viewing points, which are shown in Figs. 8(a)–8(d), respectively. The recorded experimental results confirm that a 4-view dynamic 3D display without crosstalk is successfully achieved, which is quite suitable for the multiview 3D projectors.
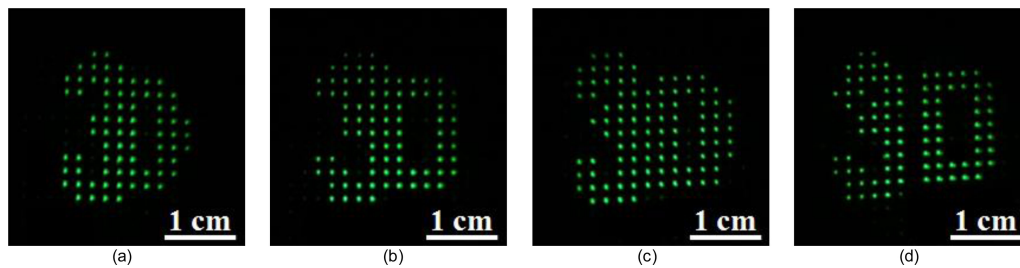
Fig. 8. (a)–(d) are the recorded reconstructed images of two characters ("3" and "D") at four different viewing points, respectively. Rotating characters, "3" and "D" (see media 9–12).

4. Discussion and Conclusions

In this paper, we propose a projection-type multiview holographic 3D display using a phase-only SLM and a directional diffractive device composed of pixelated gratings. The SLM is employed to display the phase-only Fresnel hologram of the multiview hybrid image of a 3D object for reconstructing the amplitude information of multiple 2D perspectives of the 3D object. The directional diffractive device is designed accordingly by the spatial distribution of the viewing points such that different reconstructed perspectives can be guided into different viewing zones, providing the phase information of the multiview lightfield. Furthermore, we fabricate a 4-view directional diffractive device with the designed parameters by using the pixelated holographic lithography system, and the optical properties of the fabricated directional diffractive device are measured by using the green reconstruction laser with the designed wavelength. The measurement results demonstrate that the fabricated directional diffractive device is quite suitable for the proposed multiview 3D display system to re-direct the collimated incident light into four various viewing points. Moreover, the small discrepancy between theoretical and tested angular divergence may be caused by the finite angular distribution of the input illuminating light. In addition, we construct an experimental verification system consisting of the phase-only SLM and the fabricated 4-view directional diffractive device to demonstrate a 4-view 3D display, and then several images are designed to test the performance of the system. The recorded experimental results confirm that the system can provide 3D sensation without crosstalk or ghost effect successfully. Besides, the dynamic display ability is also tested in the experiments by refreshing the adopted SLM with the sequential holograms at a refresh frame rate of 20 fps, and the captured 3D videos demonstrate that the proposed projection-type multiview holographic 3D display prototype has a promising potential for the real-time holographic 3D projectors.

There are also several quantitative indicators for evaluating the imaging quality of 3D images as follows: The first one is crosstalk, which can be defined as a proportion of the intensity of the perceived other stray perspectives to the intensity of the perceived target perspective, which mainly depends on the overlapping region of intensity distribution depicted in Fig. 4(b), and the smaller overlapping region the lower crosstalk. From Fig. 4(b), it is clearly seen that the intensity distributions between different views have no overlap, which means that the crosstalk of the experimental system is zero. The second one is resolution, which can be analyzed from two aspects. On the one hand, the resolution of the displayed image at each view can be usually expressed by the pixel number of the reconstructed perspective. In the experiment, the 4-view directional diffractive device with the total grating pixel number of 60×60 is fabricated to verify the feasibility of the proposed method such that the final each view will be consisted of 30×30 pixels. Of course the pixel number for display can be easily improved when the directional diffractive device with increasing total grating number is fabricated and the SLM with higher resolution or multiple SLMs are used. On the other hand, the image quality of optical imaging system is always determined by the impulse response of the system. Obviously, for the holographic reconstruction system based on the SLM with finite aperture, the real image of a point source should be a disc of confusion other than an ideal image point so that the resolution of the displayed image in the proposed system can also be described by

the size of the disc of confusion or the width of the impulse response. The smaller size of the disc of confusion or the width of the impulse response means the higher resolution or imaging quality of the displayed image. Furthermore, the width of the impulse response is positively correlated with the wavelength of the reconstructed light and the reconstructed distance, while negatively correlated with the aperture of the adopted SLM according to Ref. [45]. In order to obtain a higher resolution, the wavelength of the reconstructed light and the reconstructed distance need to be decreased properly and the aperture of the SLM need to be increased significantly. Based on the current available SLM, the mosaic method may be an effective approach to obtain a large aperture. The third one is energy efficiency, which mainly depends on the diffraction efficiency of the fabricated directional diffractive device in the proposed system. In the experiment, the measured diffraction efficiencies of the four convergent viewing points are all about 5% so that the energy efficiency of the fabricated directional diffractive device is about 20%. Although the current efficiencies are not very high, they are enough for the observer to clearly view the reconstructed perspectives in the ambient light, which has been previously proved by the HP Laboratories in Ref. [37]. Besides, in the proposed 3D display, the viewing angle depends on the spatial distribution of the viewing points, and the positions of the convergent viewing points relies on the diffraction angles of the diffracted light beams after modulating by the pixelated gratings in the directional diffractive device. So, the diffraction angles of the gratings need to be enlarged if the viewing angle wants to further expand. According to the grating equation, the gratings with smaller periods are required to satisfy the demand for the larger viewing angle, which provides a higher requirement for fabricating the pixelated gratings. Fortunately, the smallest period of the grating that can be fabricated by the pixelated holographic lithography could be smaller than 300 nm, which is enough for providing a large diffraction angle. Therefore, the final viewing range of 3D images can be further expanded. Moreover, we intend to optimize the diffraction efficiency of the directional diffractive device by recording the pixelated volume holographic gratings in a thick recording material. Compared with the current pixelated photoresist gratings, the first-order diffraction efficiencies of the volume gratings will be greatly improved, and the other orders will also be significantly suppressed. In addition, the complex amplitude modulation techniques or speckle noise suppressed methods can be used to optimize the image quality of the holographic reconstruction, and the chromatic multiview 3D display will also be explored in the future.

Acknowledgment

References

[1] Z. C. Fan, Y. T. Weng, G. W. Chen, and H. E. Liao, "3D interactive surgical visualization system using mobile spatial information acquisition and autostereoscopic display," *J. Biomed. Inform.*, vol. 71, pp. 154–164, May 2017.

[2] D. Zhao, L. F. Ma, C. Ma, J. Tang, and H. E. Liao, "Floating autostereoscopic 3D display with multidimensional images for telesurgical visulization," *Int. J. Comput. Assist. Radiol. Surg.*, vol. 11, no. 2, pp. 207–215, Feb. 2016.

[3] H. Yamamoto, Y. Tomiyama, and S. Suyama, "Floating aerial LED signage based on aerial imaging by retro-reflection (AIRR)," *Opt. Exp.*, vol. 22, no. 22, pp. 26919–26924, Nov. 2014.

[4] R. Hirayama *et al.*, "Design, implementation and characterization of a quantum-dot-based volumetric display," *Sci. Rep.*, vol. 5, Feb. 2015, Art. no. 8472.

[5] A. Maimone, A. Georgiou, and J. S. Kollin, "Holographic near-eye displays for virtual and augmented reality," *ACM Trans. Graphics*, vol. 36, no. 4, Jul. 2017, Art. no. 85.

[6] S. Yamada, T. Kakue, T. Shimobaba, and T. Ito, "Interactive holographic display based on finger gestures," *Sci. Rep.*, vol. 8, Jan. 2018, Art. no. 2010.

[7] J. Geng, "Three-dimensional display technologies," *Adv. Opt. Photon.*, vol. 5, no. 4, pp. 456–535, Nov. 2013.

[8] Y. J. Pan, J. Liu, X. Li, and Y. T. Wang, "A review of dynamic holographic three-dimensional display: algorithms, devices, and systems," *IEEE Trans. Ind. Inform.*, vol. 12, no. 4, pp. 1599–1610, Aug. 2016.

[9] K. Yamamoto, Y. Ichihashi, T. Senoh, R. Oi, and T. Kurita, "3D objects enlargement technique using an optical system and multiple SLMs for electronic holography," *Opt. Exp.*, vol. 20, no. 19, pp. 21137–21144, Sep. 2012.

[10] H. Sasaki, K. Yamamoto, K. Wakunami, Y. Ichihashi, R. Oi, and T. Senoh, "Large size three-dimensional video by electronic holography using multiple spatial light modulators," *Sci. Rep.*, vol. 4, Aug. 2014, Art. no. 6177.

[11] H. Yoshikawa and T. Yamaguchi, "Computer-generated holograms for 3D display," *Chin. Opt. Lett.*, vol. 7, no. 12, pp. 1079–1082, Dec. 2009.

[12] H. Pang, J. Z. Wang, A. X. Cao, M. Zhang, L. F. Shi, and Q. L. Deng, "Accurate hologram generation using layer-based method and iterative Fourier transform algorithm," *IEEE Photon. J.*, vol. 9, no. 1, Feb. 2017, Art. no. 2200108.

[13] F. Yaras, H. Kang, and L. Onural, "State of the art in holographic displays: a survey," *J. Disp. Technol.*, vol. 6, no. 10, pp. 443–454, Oct. 2010.

[14] G. Li, J. Jeong, D. Lee, J. Yeom, C. Jang, S. Lee, and B. Lee, "Space bandwidth product enhancement of holographic display using high-order diffraction guided by holographic optical element," *Opt. Exp.*, vol. 23, no. 26, pp. 33170–33183, Dec. 2015.

[15] M. Agour, C. Falldorf, and R. B. Bergmann, "Holographic display system for dynamic synthesis of 3D light fields with increased space bandwidth product," *Opt. Exp.*, vol. 24, no. 13, pp. 14393–14405, Jun. 2016.

[16] K. Wakunami *et al.*, "Projection-type see-through holographic three-dimensional display," *Nature Commun.*, vol. 7, Oct. 2016, Art. no. 12954.

[17] J. Hahn, H. Kim, Y. Lim, G. Park, and B. Lee, "Wide viewing angle dynamic holographic stereogram with a curved array of spatial light modulators," *Opt. Exp.*, vol. 16, no. 16, pp. 12372–12386, Aug. 2008.

[18] F. Yaras, H. Kang, and L. Onural, "Circular holographic video display system," *Opt. Exp.*, vol. 19, no. 10, pp. 9147–9156, May 2011.

[19] T. Kozacki, M. Kujawińska, G. Finke, B. Hennelly, and N. Pandey, "Extended viewing angle holographic display system with tilted SLMs in a circular configuration," *Appl. Opt.*, vol. 51, no. 11, pp. 1771–1780, Apr. 2012.

[20] Y.-Z. Liu, X.-N. Pang, S. J. Jiang, and J.-W. Dong, "Viewing-angle enlargement in holographic augmented reality using time division and spatial tiling," *Opt. Exp.*, vol. 21, no. 10, pp. 12068–12076, May 2013.

[21] Y. Sando, D. Barada, and T. Yatagai, "Holographic 3D display observable for multiple simultaneous viewers from all horizontal directions by using a time division method," *Opt. Lett.*, vol. 39, no. 19, pp. 5555–5557, Oct. 2014.

[22] N. A. Dodgson, "Autostereoscopic 3D displays," *Computer*, vol. 38, no. 8, pp. 31–36, Aug. 2005.

[23] Y.-C. Chang, T.-H. Jen, C.-H. Ting, and Y.-P. Huang, "High-resistance liquid-crystal lens array for rotatable 2D/3D autostereoscopic display," *Opt. Exp.*, vol. 22, no. 3, pp. 2714–2724, Feb. 2014.

[24] J.-L. Feng, Y.-J. Wang, S.-Y. Liu, D.-C. Hu, and J.-G. Lu, "Three-dimensional display with directional beam splitter array," *Opt. Exp.*, vol. 25, no. 2, pp. 1564–1572, Jan. 2017.

[25] G.-J. Lv, J. Wang, W.-X. Zhao, and Q.-H. Wang, "Three-dimensional display based on dual parallax barriers with uniform resolution," *Appl. Opt.*, vol. 52, no. 24, pp. 6011–6015, Aug. 2013.

[26] W.-X. Zhao, Q.-H. Wang, A.-H. Wang, and D.-H. Li, "Autostereoscopic display based on two-layer lenticular lenses," *Opt. Lett.*, vol. 35, no. 24, pp. 4127–4129, Dec. 2010.

[27] Q.-H. Wang, C.-C. Ji, L. Li, and H. Deng, "Dual-view integral imaging 3D display by using orthogonal polarizer array and polarization switcher," *Opt. Exp.*, vol. 24, no. 1, pp. 9–16, Jan. 2016.

[28] K.-W. Chien and H.-P. D. Shieh, "Time-multiplexed three-dimensional displays based on directional backlights with fast-switching liquid-crystal displays," *Appl. Opt.*, vol. 45, no. 13, pp. 3106–3110, May 2006.

[29] C.-H. Ting, Y.-C. Chang, C.-H. Chen, Y.-P. Huang, and H.-W. Tsai, "Multi-user 3D film on a time-multiplexed side-emission backlight system," *Appl. Opt.*, vol. 55, no. 28, pp. 7922–7928, Oct. 2016.

[30] Y. Takaki and N. Nago, "Multi-projection of lenticular displays to construct a 256-view super multi-view display," *Opt. Exp.*, vol. 18, no. 9, pp. 8824–8835, Apr. 2010.

[31] C.-K. Lee, S.-G. Park, S. Moon, J.-Y. Hong, and B. Lee, "Compact multi-projection 3D display system with light-guide projection," *Opt. Exp.*, vol. 23, no. 22, pp. 28945–28959, Nov. 2015.

[32] C.-K. Lee, S.-G. Park, S. Moon, and B. Lee, "Viewing zone duplication of multi-projection 3D display system using uniaxial crystal," *Opt. Exp.*, vol. 24, no. 8, pp. 8458–8470, Apr. 2016.

[33] S. Tay *et al.*, "An updatable holographic three-dimensional display," *Nature*, vol. 451, no. 7179, pp. 694–698, Feb. 2008.

[34] P.-A. Blanche *et al.*, "Holographic three-dimensional telepresence using large-area photorefractive polymer," *Nature*, vol. 468, no. 7320, pp. 80–83, Nov. 2010.

[35] M. Lucente and T. A. Galyean, "Rendering interactive holographic images," in *Proc. 22nd Annu. Conf. Comput. Graph. Interact. Techn.*, Los Angeles, CA, USA, Aug. 1995, pp. 387–394.

[36] J. H. Kulick *et al.*, "Partial pixels: A three-dimensional diffractive display architecture," *J. Opt. Soc. Amer. A*, vol. 12, no. 1, pp. 73–83, Jan. 1995.

[37] D. Fattal *et al.*, "A multi-directional backlight for a wide-angle, glasses-free three-dimensional display," *Nature*, vol. 495, no. 7441, pp. 348–351, Mar. 2013.

[38] W. Q. Wan *et al.*, "Efficient fabrication method of nano-grating for 3D holographic display with full parallax views," *Opt. Exp.*, vol. 24, no. 6, pp. 6203–6212, Mar. 2016.

[39] W. Q. Wan *et al.*, "Multiview holographic 3D dynamic display by combining a nano-grating patterned phase plate and LCD," *Opt. Exp.*, vol. 25, no. 2, pp. 1114–1122, Jan. 2017.

[40] J. Goodman, *Introduction to Fourier Optics*. New York, NY, USA: McGraw-Hill, 1996, pp. 32–55.

[41] J. E. Harvey and C. L. Vernold, "Description of diffraction grating behavior in direction cosine space," *Appl. Opt.*, vol. 37, no. 34, pp. 8158–8160, Dec. 1998.

[42] D. Palima and V. R. Daria, "Holographic projection of arbitrary light patterns with a suppressed zero-order beam," *Appl. Opt.*, vol. 46, no. 20, pp. 4197–4201, Jul. 2007.

[43] H. Zhang, J. H. Xie, J. Liu, and Y. T. Wang, "Elimination of a zero-order beam induced by a pixelated spatial light modulator for holographic projection," *Appl. Opt.*, vol. 48, no. 30, pp. 5834–5841, Oct. 2009.

[44] M. Agour, E. Kolenovic, C. Falldorf, and C. V. Kopylow, "Suppression of higher diffraction orders and intensity improvement of optically reconstructed holograms from a spatial light modulator," *J. Opt. A, Pure Appl. Opt.*, vol. 11, Aug. 2009, Art. no. 105405.

[45] J. C. Li, H.-Y. Tu, W.-C. Yeh, J. B. Gui, and C.-J. Cheng, "Holographic three-dimensional display and hologram calculation based on liquid crystal on silicon device [invited]," *Appl. Opt.*, vol. 53, no. 27, pp. G222–G231, Sep. 2014.